Available online at www.sciencedirect.com
ScienceDirect
Journal of Environmental Sciences 2011, 23(5) 790–797
JOURNAL OF ENVIRONMENTAL SCIENCES
ISSN 1001-0742
CN 11-2629/X
www.jesc.ac.cn

Applying model simulation and photochemical indicators to evaluate ozone sensitivity in southern Taiwan

Yen-Ping Peng[1], Kang-Shin Chen[2], Hsin-Kai Wang[2], Chia-Hsiang Lai[3,*], Ming-Hsun Lin[4], Cheng-Haw Lee[4]

1. Graduate Institute of Environmental Engineering, "National" Taiwan University, Taipei 106, Taiwan, China. E-mail: yppeng@ntu.edu.tw
2. Institute of Environmental Engineering, National Sun Yat-Sen University, Kaohsiung 804, Taiwan, China
3. Department of Health Safety and Environmental Engineering Central Taiwan University of Science and Technology, Taichung 406, Taiwan, China
4. Department of Resources Engineering, National Cheng-Kung University, Tainan 701, Taiwan, China

Received 23 June 2010; revised 01 December 2010; accepted 08 December 2010

Abstract

Ozone sensitivity was investigated using CAMx simulations and photochemical indicator ratios at three sites (Pingtung City, Chao-Chou Town, and Kenting Town) in Pingtung County in southern Taiwan during 2003 and 2004. The CAMx simulations compared fairly well with the hourly concentrations of ozone. Simulation results also showed that Pingtung City was mainly a volatile organic compounds (VOC)-sensitive regime, while Chao-Chou Town was either a VOC-sensitive or a NO*x*-sensitive regime, depending on the seasons. Measurements of three photochemical indicators (H_2O_2, HNO_3, and NO*y*) were conducted, and simulated three transition ranges of H_2O_2/HNO_3 (0.5–0.8), O_3/HNO_3 (10.3–16.2) and O_3/NO*y* (5.7–10.8) were adopted to assess the ozone sensitive regime at the three sites. The results indicated that the three transition ranges yield consistent results with CAMx simulations at most times at Pingtung City. However, both VOC-sensitive and NO*x*-sensitive regimes were important at the rural site Chao-Chou Town. Kenting Town, a touring site at the southern end of Taiwan, was predominated by a NO*x*-sensitive regime in four seasons.

Key words: photochemical indicator; ozone sensitivity; volative organic compounds; NO*x*; CAMx

DOI: 10.1016/S1001-0742(10)60479-2

Citation: Peng Y P, Chen K S, Wang H K, Lai C H, Lin M H, Lee C H, 2011. Applying model simulation and photochemical indicators to evaluate ozone sensitivity in southern Taiwan. Journal of Environmental Sciences, 23(5): 790–797

Introduction

Nitrogen oxides (NO*x* = NO + NO_2) and volatile organic compounds (VOC) play important roles in ozone formation. Accumulation of ozone near the ground is influenced by physical and chemical processes and by meteorological conditions (NRC, 1991; Hwang et al., 2007). The current state of progress in measurement, analysis and modeling of ozone precursors, photochemical behavior, and transport processes has been recently reviewed (Blanchard, 2000; Hidy, 2000; Lin, 2008; Lal et al., 2009; Liu and Leung, 2008; Peng et al., 2006; Russell and Dennis, 2000; Sillman, 1999; Trainer et al., 2000). In the non-attainment area, photochemical models are often employed to predict hourly ozone variations and thus help establish cost-effective means of reducing ambient ozone to control the emissions of VOC and NO*x* from various sources. Another approach for investigation of ozone-VOC-NO*x* sensitivity is to use photochemical indicator species or species ratios, such as hydrogen peroxide and reactive nitrogen species (Milford et al., 1994; Sillman et al., 1997). Comparisons between model predictions and measured values for the indicator species would also provide a test of the accuracy of model sensitivity predictions (Peng et al., 2006; Sillman, 1995).

Pingtung County is in the southern end of Taiwan, with around 0.91 million inhabitants and an area of 2775 km^2. It is mainly agricultural, with touring and sightseeing (e.g., at Kenting Town), except for some densely populated areas in Pingtung City (Northern part) and Chao-Chou Town (Central part), with several small-sized industrial parks. Taiwan-EPA (Environmental Protection Administration) divides Taiwan into seven airbasins. Pingtung County belongs to the Kao-Ping airbasin, which has the worst air quality in Taiwan (Liu, 2007). The ozone episodes (> 120 ppb) often occur in Pingtung City and Chao-Chou Town, but barely occurs at Kenting Town. This is mainly because the northern and central parts of Pingtung County are south of, and thus downwind of, the Kaohsiung areas (Kaohsiung City and Kaohsiung County), whenever a northerly or north-easterly wind prevails, such as in autumn and winter (Chen et al., 2003, 2004). Photochemical simulations by Chen et al. (2003) showed that about 50%–60% of

* Corresponding author. E-mail: chlai2@ctust.edu.tw

the ambient ozone in Pingtung County were transported from and/or contributed by Kaohsiung area, depending on the season. The simulations also showed that most of concentrations of the ambient ozone in Kaohsiung City and Pingtung City were sensitive to the reduction of VOC emissions.

In this work, simulations using the CAMx-2.0 (ENVIRON, 1998) were conducted for four ozone episodes in the Pingtung County, each covering three consecutive days (or 72 hr). The potential influence of initial and boundary conditions on the model performance was assessed. The sensitivity analysis of ozone concentrations to emission reductions in NO*x* and VOC was performed. Meanwhile, atmospheric concentrations of H_2O_2, HNO_3 and reactive nitrogen (NO*y*) were measured at three sites in Pingtung County in four seasons during 2003–2004. The VOC- or NO*x*-sensitive regime to the formation of ozone was identified at each site using both CAMx simulations and ratios of photochemical indicators.

1 Experiment

1.1 Sampling sites and periods

Three sampling sites, Pingtung City, Chao-Chou Town and Kenting Town were chosen, representing the northern, central, and southern parts in Pingtung County, respectively (Fig. 1). Hourly air quality data and meteorological conditions were available at the three sites, operated by Taiwan-EPA, including concentrations of O_3 and NO*x*, temperature, and wind. The distances are approximately 18 km between Pingtung City and Chao-Chou Town and 70 km between Chao-Chou and Kenting Towns.

Samples were taken on five days in four seasons in 2003 and 2004. Samples of H_2O_2, HNO_3 and NO*y* were collected concurrently for eight 1-hr periods between 09:00 and 17:00 at Pingtung, Chao-Chou and Kenting. Table 1 presents the meteorological conditions at the three monitoring sites, including temperature, wind speed and period of sunshine during the period of study.

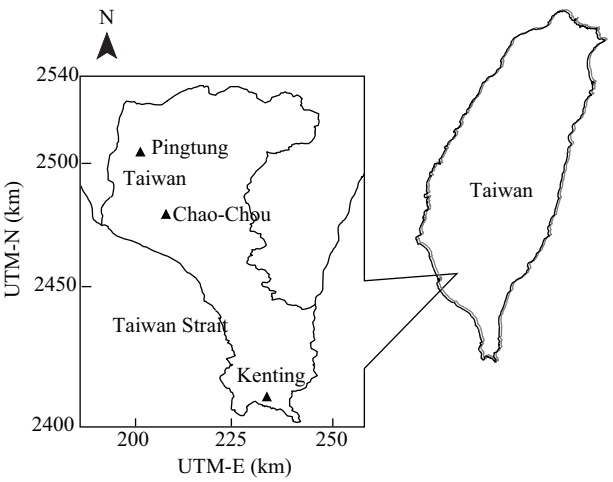

Fig. 1 Model domain and three measurement sites in Pingtung County, Southern Taiwan.

1.2 Sampling and analysis of H_2O_2

Gaseous samples were collected in two identical midget fritted glass bubblers (Supelco No. 6-438), each containing 15 mL of $TiOSO_4$ collecting solution. The inlet of the first bubbler had two ports: one port was connected to the inlet of the second bubbler, and the other was connected to the outlet of an air sampler, via silica gel tubes. Desiccants were packed in the tube between the first bubbler and an air pump (SKC Model 210-1000s) operated at a flow rate of 500 mL/min. The sampling and analytical procedures complied with US-OSHA (Occupational Safety and Health Administration) Method VI-6. The Ti-H_2O_2 solution was analyzed in the laboratory using a spectrophotometer (Shimadzu UV-160, Japan) at a wavelength of 410 nm. No breakthrough of the species occurred in the test tubes. Calibrations were conducted using seven concentrations of standard samples, with a coefficient of determination, R^2, of above 0.997. The detection limit of H_2O_2 was 0.12 ppb.

1.3 Sampling and analysis of HNO_3

Gaseous samples of HNO_3 were collected using silica gel adsorption tubes (SKC No. 226-10-03) of length 11 cm and outer diameter 7 mm, containing a 400-mg front section and a 200-mg backup section of washed silica gel, with flamed-sealed ends. The adsorption tube was connected to a pump (SKC No. 210-1002MH) operated at an airflow rate of 250 mL/min. No breakthrough of the compounds occurred in the tubes. The sampling and analytical procedures complied with US-NIOSH (The National Institute for Occupational Safety and Health) Method 7903. The samplers were analyzed in the laboratory using ion chromatography (DIONEX Model DX-100) with an AS-4ASC separator column of 4 mm. Calibrations were conducted using seven concentrations of standard samples, with a coefficient of determination, $R^2 > 0.997$. The detection limit of HNO_3 was 1.55 ppb.

1.4 Sampling and analysis of NO*y*

Reactive nitrogen, NO*y*, refers to total reactive nitrogen including NO, NO_2, HNO_3, HNO_2, PAN and alky nitrates. Concentration of ambient NO*y* was converted to concentration of NO via molybdenum catalyst converter at 350°C with low influence from NH_3 or other species (Williams, 1995; Honrath and Jaffe, 1990; Fehsenfeld et al., 1987). The ground molybdenum was put in a glass tube (length = 15 cm, diameter = 3 cm) with quartz wool in both end and heated to 350°C by temperature controller. Inlet NO*y* was converted to NO under the molybdenum catalysis. Outlet NO gaseous was connected to an ambient NO detector (Ecotech, Model 1070). The convertibility of NO*y* to NO was about 93.8%. The detection limit was 0.1 ppb for both NO and NO*y* (Delany et al., 1982; Dickerson et al., 1984).

2 Modeling

The full horizontal domain is 160 km long and 120 km wide and includes a 40×30 horizontal coarse grid of

Table 1 Meteorological conditions at Pingtung City (P.T.), Chao-Chou Town (C.C.) and Kenting Town (K.T.) during the study period

Date (d/m/yr)	Temperature (°C)			Wind speed (m/sec)			Period of sunshine (hr)		
	P.T.	C.C.	K.T.	P.T.	C.C.	K.T.	P.T.	C.C.	K.T.
7/8/2003	29.5	28.7	26.7	1.8	1.4	4.8	11.3	7.8	7.8
8/8/2003	29.7	28.9	27.0	1.5	1.1	6.1	9.5	9.1	9.1
9/8/2003	30.2	28.4	27.0	1.2	0.9	3.8	9.3	9.8	9.8
10/8/2003	30.5	28.9	27.0	1.3	0.8	2.9	6.6	8.0	8.0
11/8/2003	29.7	28.3	26.4	1.8	1.8	3.0	9.6	5.7	5.7
9(20)/11/2003	26.5	28.0	26.6	0.8	0.8	3.6	9.2	7.7	8.7
10(21)/11/2003	26.5	27.5	25.6	1.0	0.9	6.2	6.6	4.2	4.0
11(22)/11/2003	24.9	22.4	24.1	0.9	0.8	12.9	3.2	0	6.2
12(23)/11/2003	23.2	24.0	23.3	0.7	0.7	11.5	2.1	0	9.5
13(24)/11/2003	23.0	25.7	22.8	0.6	0.7	11.0	8.2	7.7	7.3
13/1/2004	16.9	18.8	17.1	1.0	1.2	10.3	0.4	0.7	0.7
14/1/2004	18.7	20.0	18.7	1.0	1.0	8.0	9.3	5.4	5.4
15/1/2004	19.4	20.7	21.0	0.9	1.0	5.9	9.3	5.5	5.5
16/1/2004	21.2	22.9	22.6	1.6	1.8	3.6	8.9	5.7	5.7
17/1/2004	19.3	20.6	20.4	1.0	1.1	8.6	6.2	7.8	7.8
5/3/2004	20.4	22.0	20.3	1.4	1.4	5.5	8.1	7.0	7.0
6/3/2004	19.9	21.5	19.8	0.8	1.1	13.7	0.4	3.1	3.1
7/3/2004	18.7	20.3	16.5	0.8	0.9	13.0	0.6	0.4	0.4
8/3/2004	18.7	19.5	18.5	1.1	1.1	7.9	10.6	7.7	7.7
9/3/2004	20.0	21.2	19.5	1.2	1.0	5.1	10.6	8.9	8.9

Autumn samplings in Chao-Chou were performed on 20–24 November in 2003 due to the EPA monitoring site at Chao-Chou was undergoing maintenance on 9–13 November in 2003.
Temperatures and wind speeds are daily means. Period of sunshine represents the sum of sunshine hour for solar irradiation above 120 W/(m^2·hr).

4×4-km cells (Fig. 2). To save computational time while improving spatial resolution, a smaller 24 × 32 grid of 1×1-km cells is nested in the coarse grids to cover the target area. Six vertical layers are considered, with the layer interfaces at 50, 150, 600, 900, 1500, and 3000 m, respectively.

It simulates the emission, dispersion and removal of inert and chemically reactive pollutants in the lower troposphere by solving the pollutant continuity equation for chemical species (l) within each grid cell in a system of nested 3D grids. The species continuity equation is expressed in terrain-following height (z) coordinates as:

$$\frac{\partial c_l}{\partial t} = -\left(\nabla_H \cdot \overrightarrow{V_H} c_l\right)\Big|_{\text{horizontal advection}} + \left[\frac{\partial (c_l \eta)}{\partial z} - c_l \frac{\partial^2 h}{\partial z \partial t}\right]\Big|_{\text{vertical transport}} + (\nabla \cdot K \nabla c_l)\,|_{\text{turulent diffusion}} + \frac{\partial c_l}{\partial t}\Big|_{\text{chemistry}} + \frac{\partial c_l}{\partial t}\Big|_{\text{emission}} + \frac{\partial c_l}{\partial t}\Big|_{\text{removal}} \quad (1)$$

where, c_l (t) is the concentration of species l as a function of space (x, y, z) and time t, V_H is the horizontal wind vector, η is the vertical entrainment rate, h is the layer interface height, and K is the turbulent exchange coefficients. The rates of chemical production, emission and removal of species l are also considered. Three statistical quantities were employed to measure the performance of each tested case. These are the coefficient of determination, R^2, the correlation coefficient, R, and the "index of agreement", d_1; according to (Willmott et al., 1985):

$$d_1 = 1 - \frac{\sum_{i=1}^{N} (|P_i - O_i|)}{\sum_{i=1}^{N} \left(\left|P_i - \overline{O}\right| + \left|O_i - \overline{O}\right|\right)} \quad (2)$$

where, P_i and O_i are the predicted and measured values, respectively, with a sample size N; and $\overline{O}$ is the average of all measured data. Note that the coefficient of variation of prediction, s; equals the standard deviation of the predictions with respect to the measured data divided by the mean value of the measured data.

3 Results and discussion

3.1 CAMx simulation results

Figure 2a and b presents the selected ground-level ozone contours at 10:00 and 14:00, respectively, on 9 November 2003, which had the highest concentration of ozone (approximately 139 ppb) during the study period. Figure 2a shows that the concentration of ozone was 70–90 ppb in northern part, 40–50 ppb in central part, and 20 ppb in southern part of Pingtung County at 10 a.m., at which time the sunlight was weak and the outdoor temperature had just started to rise. However, Fig. 2b shows that the concentration of ozone rose to 100–120 ppb at 14:00, covering the northwest part of Pingtung County. Meanwhile, the ozone concentration in the southern part of Kaohsiung City also increased to 120 ppb. This ozone episode was related to low wind (< 4 m/sec) and high period of sunshine (> 7.5 hr), as shown in Table 1. The above simulation results are compared to the hourly ozone data at the three monitoring sites, and are displayed in Figures 3a–c, respectively. Figure 3a, b shows that 11:00 to 16:00 is the period during which ozone concentration usually exceeds 80 ppb. Both simulated and measured peak ozone occurs at 12:00–14:00 when sunlight and ambient temperature are highest in the day; however, the simulated peak ozone concentrations were slightly higher (6–31 ppb) than measured values. On the contrary, due to the model setting of background ozone concentration (30 ppb), the

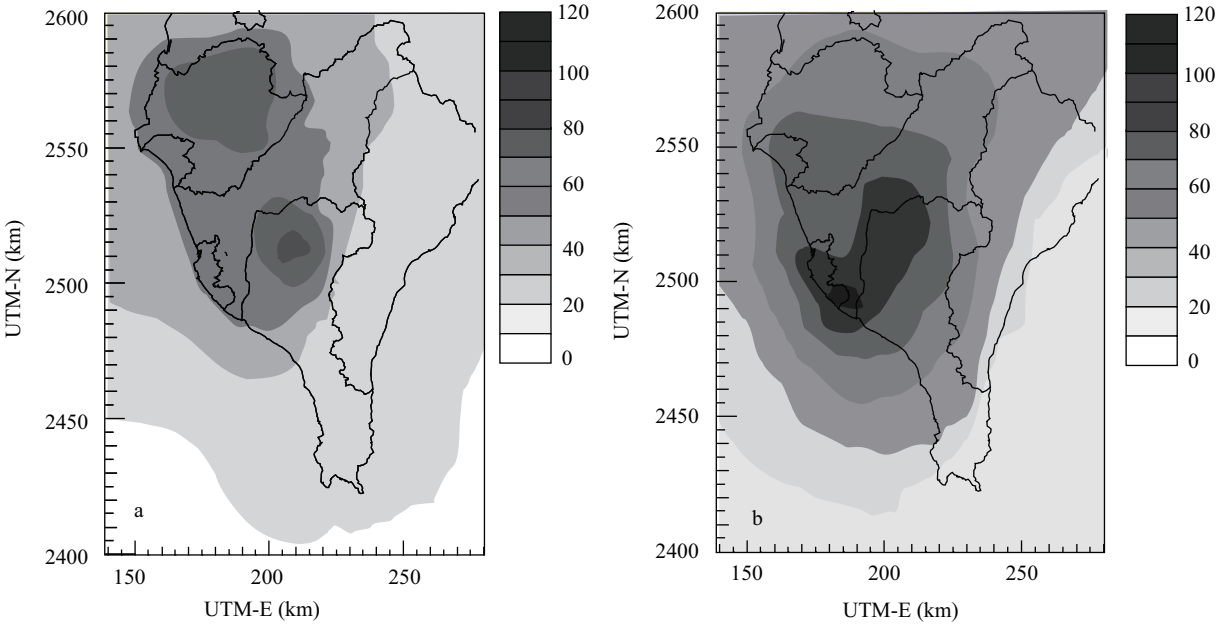

Fig. 2 Selected ground-level simulated ozone contours (ppb) at 10:00 (a) and 14:00 (b) on 9 November 2003 using CAMx model.

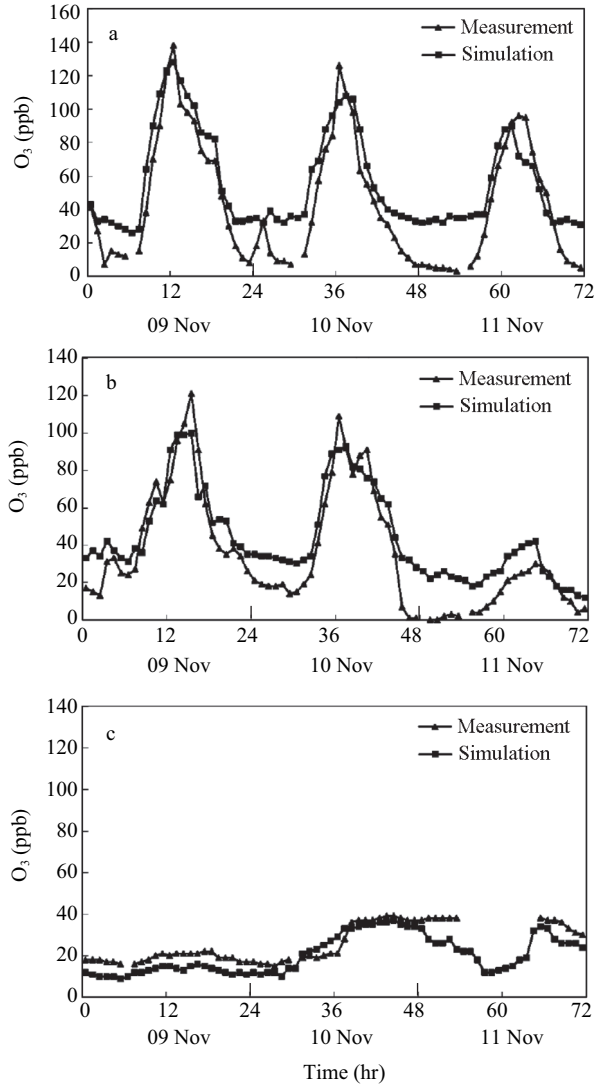

Fig. 3 Comparisons of hourly ozone concentrations during 2003 autumn episodes at Pingtung City (a), Chao-Chou Town (b), and Kenting Town (c).

measured ozone concentrations were higher than simulated values. The comparisons of hourly ozone concentrations in summer, winter and spring were similar to the results in autumn. Figure 3 also shows that simulations agree fairly well with measurements. Statistic results of model performance were presented below.

Table 2 summaries the performance results of CAMx simulations for three consecutive days at the three sites in four seasons (N = 216). The correlation coefficients (R) between measured and simulated values are 0.79, 0.89, 0.89 and 0.90 in summer, autumn, winter and spring, respectively. The index of agreement (d_1), representing the difference between predictions and measurements, are 0.63, 0.70, 0.68 and 0.74 in summer, autumn, winter and spring, respectively. According to Hurley et al. (2003a, 2003b) the agreement between prediction and measurement is regarded as good when d_1 exceeds 0.5.

3.2 Ozone-NO*x*-VOC sensitivity analysis

The sensitivity of ambient ozone to anthropogenic emissions of NO*x* and VOC can be studied by running a model of the base case but with reduced NO*x* or VOC while keeping biogenic VOC emission unchanged and by examining the predicted response in terms of ozone concentration (Chen et al., 2003; Milford et al., 1989; Roselle et al., 1995). Since the ozone concentrations were usually low (< 40 ppb) at Kenting Town (a touring site at the southern end of Taiwan), no ozone sensitivity simulation

Table 2 Statistical results of model performance in four seasons

Season	R^2	R	d_1
summer	0.62	0.79	0.63
autumn	0.80	0.89	0.70
winter	0.79	0.89	0.68
spring	0.82	0.90	0.74

R^2 is the coefficient of determinant (0 to 1); R is the correlation coefficient (0 to ±1); and d_1, defined in Eq. (2), is the index of agreement (0 to 1).

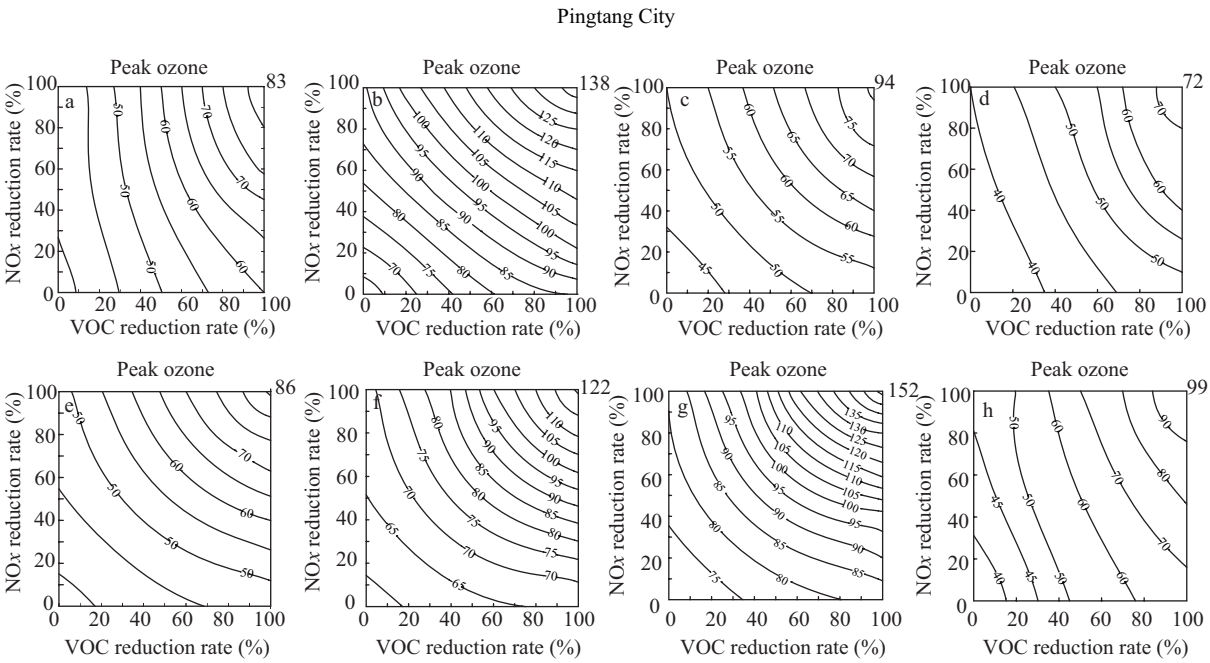

Fig. 4 Simulations of peak ozone to reductions in VOC and NO*x* emissions at Pingtung City in summer (a), autumn (b), winter (c), spring (d); and at Chao-chou Town in summer (e), autumn (f), winter (g), spring (h) in 2003–2004.

was performed. Figure 4 shows the simulated peak ozone responses at the Pingtung City and Chao-Chou Town. Figure 4 a–h shows that peak O_3 concentration decreases as NO*x* or VOC emission is reduced. For the episodes at Pingtung City, results show VOC sensitive for emission reductions in summer, winter and, spring (Fig. 4a, c, d). Take Fig. 4a for example, the peak ozone concentration could be reduced from 83 to 70 ppbv through two ways, one is to reduce 29% VOC and the other is to reduce 53% NO*x*. Meanwhile, the results show slightly NO*x*-sensitive or a mixed (i.e., equally important) regime in autumn (Fig. 4b). For the episodes at Chao-Chou Town, results show slightly NO*x*-sensitive for emission reductions in summer, autumn and winter (Fig. 4f–h), but VOC-sensitive in spring (Fig. 4e). Therefore, the present results are consistent with Sillman's results (Sillman, 1999), indicating that VOC-sensitive chemistry usually occurs for moderate reductions (25%–50%) in VOC and NO*x* concentrations and that NO*x*-sensitive chemistry occurs for larger percentage reductions. Notably, freshly emitted pollutants are typically (though not always) characterized by VOC-sensitive chemistry and evolve towards NO*x*-sensitive chemistry as the air mass moves downwind. Pingtung City is likely to be in a VOC-sensitive regime because it is relatively dense populated than at the downwind site Chou-Chou Town.

3.3 Transition ranges of photochemical indicator ratios

Comparisons between measured photochemical indicator ratios and ozone reduction simulations, corresponding to 35% VOC reduction and 35% NO*x* reduction according to Sillman et al. (1995) were made. The model time period of O_3 were the same with the measured time period of photochemical indicator species. Three plots in Figure 5 shows the ranges of indicator values associated with VOC-sensitive and NO*x*-sensitive locations, defined

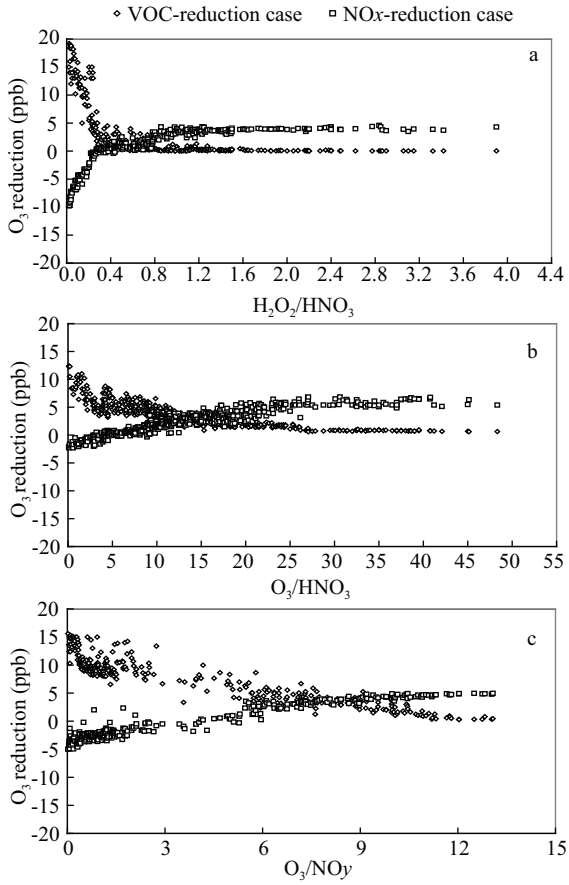

Fig. 5 Predicted reduction of simulated O_3 resulting from 35% VOC reduction and 35% NO*x* reduction vs. measured indicator values. (a) H_2O_2/HNO_3; (b) O_3/HNO_3; (c) O_3/NOy at Pingtung City, southern Taiwan.

as the locations where the simulated reduction in peak ozone associated with reduced NO*x* exceeds the simulated reduction associated with reduced VOC > 5 ppb (Sillman, 1995). Remarks are in order below.

Figure 5a shows reductions in VOC have positive impact on O_3 concentration in locations where H_2O_2/HNO_3 < 0.2, but the reduction in O_3 associated with reduced NOx increases with increasing H_2O_2/HNO_3. The overlap between VOC- and NOx-sensitive locations takes place at a value of H_2O_2/HNO_3 of approximately 0.5–0.8. Among all photochemical indicators, the ratio of hydrogen peroxide to nitric acid shows stronger relation to the connection between VOC-NOx sensitivity in terms of both theory and simulation results. The transition from NOx-sensitive to VOC-sensitive chemistry is linked with the replacement of peroxides by nitric acid as the dominant sink for odd hydrogen, and therefore by a decreasing ratio of O_3 to reactive nitrogen (Sillman, 1995; Jimenez and Baldasano, 2004).

Figure 5b shows that the model predicts the crossover between NOx- and VOC-sensitive ozone occurs at O_3/HNO_3 of 10.3–16.2. The correlation between O_3/HNO_3 and NOx-VOC chemistry is also based on odd hydrogen chemistry, OH + $NO_2 \longrightarrow HNO_3$. The formation of nitric acid represents the major sink for odd hydrogen, and then the equation of odd hydrogen sources and sinks demonstrates that OH must decrease with increasing NOx. OH will also increase slightly with increasing VOC, reflecting the role of the latter as sources of odd hydrogen.

The uses of O_3/NOy as a photochemical indicator for ozone sensitivity were discussed in detail in many studies (Milford et al., 1994; Sillman et al., 1997; Sillman, 1995; Jimenez and Baldasano, 2004). In addition, the association of ozone sensitivity with O_3/NOy reflects a feature of photochemical evolution that is independent of initial VOC/NOx ratios. Figure 5c shows that low O_3/NOy is associated with VOC-sensitive ozone, a result that parallels the relation between ozone sensitivity and VOC/NOx. Transition regime of O_3/NOy is achieved between 5.7–10.8 derived from simulations.

Sillman et al. (1995) proposed that in most case the 95th percentile VOC-sensitive value is lower than the 5th percentile NOx-sensitive value. This comparison between 95th and 5th percentiles identifies the indicator values associated with the transition between VOC-sensitive and NOx-sensitive chemistry. Table 3 shows the simulated transition ranges.

3.4 Ozone sensitivity determined by indicator ratios

The transition range (or threshold values) of H_2O_2/HNO_3: 0.49–0.77, O_3/HNO_3: 10.32–16.17, and O_3/NOy: 5.70–10.78, were then adopted to assess a VOC-sensitive or an NOx-sensitive regime to ozone formation, in which a lower value than the threshold ratio indicates a VOC-sensitive regime, a higher value than the threshold ratio indicates a NOx-sensitive regime, and otherwise indicates an intermediate (or a transition) regime. Table 4 summaries the percentages of VOC-sensitive and NOx-sensitive regimes to ozone formation at the three sites in four seasons using the three indicator ratios.

All indicator ratios show that Pingtung City was dominated by a VOC-sensitive regime in four seasons. These are consistent with the CAMx simulations, indicating VOC sensitive in summer, winter, and spring, except being a slightly NOx-sensitive or a mixed regime in autumn. However, some conflicting results appeared at Chao-Chou Town. For example, the percentages of NOx-sensitive regimes exceed those of VOC-sensitive regimes using all ratios in summer; the intermediate (transition) regime appears relatively frequently at Chao-Chou. In contrary, the percentages of VOC-sensitive regimes exceed those of NOx-sensitive regimes in autumn, winter and spring using the ratios of H_2O_2/HNO_3, O_3/HNO_3 and O_3/NOy at Chao-

Table 3 Distribution of photochemical indicator values for VOC-sensitive and NOx-sensitive chemistry

Indicator	VOC-sensitive location		NOx-sensitive location	
	50th percentile	95th percentile	5th percentile	50th percentile
H_2O_2/HNO_3	0.32	0.49	0.77	1.25
O_3/HNO_3	6.11	10.32	16.17	31.00
O_3/NOy	1.53	5.70	10.78	11.66
NOy	67.50	31.00	10.40	3.40

Table 4 Percentages of VOC and NOx-sensitive regimes to ozone formation according to threshold ratios at the three sites in four seasons in 2003–2004

Site	Season	H_2O_2/HNO_3		O_3/HNO_3		O_3/NOy	
		VOC-sensitive (< 0.5)	NOx-sensitive (> 0.8)	VOC-sensitive (< 10.3)	NOx-sensitive (> 16.2)	VOC-sensitive (< 5.7)	NOx-sensitive (> 10.8)
Pingtung	Summer	67.8	12.5	50.0	14.2	100	0
	Autumn	84.3	2.0	52.0	14.2	100	0
	Winter	80.8	3.8	86.5	7.7	100	0
	Spring	84.7	3.8	80.8	9.6	100	0
Chao-Chou	Summer	25.0	51.8	32.1	44.6	5.4	14.7
	Autumn	52.4	22.6	49.2	27.8	100	0
	Winter	62.2	17.0	56.6	18.9	100	0
	Spring	47.1	29.4	42.0	36.0	96.1	0
Kenting	Summer	34.0	42.0	5.4	57.1	12.5	53.7
	Autumn	17.0	67.9	0	78.7	17.0	48.5
	Winter	12.0	68.0	8.2	45.9	12.8	30.8
	Spring	27.5	50.9	0	64.7	18.2	18.2

Chou. Similar results were observed by Peng et al. (2006) using the different threshold values of H_2O_2/HNO_3: 0.3–0.6, O_3/HNO_3: 12–6 and *E* (extent of reaction). 0.6–0.8 (smog production model) to evaluate the ozone sensitive chemistry at Chao-Chou Town, indicating that Chao-Chou was VOC sensitive in winter, but NO*x* sensitive in spring. Thus, all these suggest that both VOC-sensitive and NO*x*-sensitive regimes are important at the rural site Chao-Chou Town. Finally, Kenting Town was predominated by a NO*x*-sensitive regime for all indicator ratios in four seasons.

It is interesting to see whether the measured indicator ratios in high O_3 concentrations differ from those in low O_3 concentrations. Table 5 shows that all indicator ratios are weekly correlated with O_3 concentration during both high (> 80 ppb) and low (< 80 ppb) ozone periods, since the correlation coefficients, *R*, are very small and within –0.28 to 0.38. Trainer et al. (1993) also found weak correlations between O_3 and NO*y*. Therefore, the indicator ratios investigated by various researchers (Milford et al., 1994; Sillman et al., 1997; Sillman, 1995; Jimenez and Baldasano, 2004) are appropriate for studying O_3-NO*x*-VOC sensitivity.

Table 5 Relationships between indicator species and O_3 concentration during low and high ozone periods

	Correlation coefficient (*R*)	
	Low ozone period (< 80 ppb)	High ozone period (> 80 ppb)
H_2O_2 vs. O_3	0.23	–0.20
HNO_3 vs. O_3	0.29	0.28
NO*y* vs. O_3	–0.28	0.05
H_2O_2/HNO_3 vs. O_3	–0.0007	–0.02
O_3/HNO_3 vs. O_3	0.38	0.14
O_3/NO*y* vs. O_3	0.25	0.12

4 Conclusions

Ozone sensitivity was examined using CAMx model and *in-situ* measured photochemical indicators in Pingtung County, southern Taiwan, in four seasons during 2003 and 2004. Simulations of hourly ozone concentrations agree reasonably well with measurements. Simulations of ozone-NO*x*-VOC sensitivity show a VOC-sensitive regime for emission reductions at Pingtung City. At Chao-Chou Town, simulation results show NO*x*-sensitive for emission reductions in summer, autumn and winter, but a VOC-sensitive regime in spring.

The threshold ratios of H_2O_2/HNO_3 (0.5–0.8), O_3/HNO_3 (10.3–16.2) and O_3/NO*y* (5.7–10.8) yield consistent results with CAMx simulations at most times at Pingtung City, except that in autumn. However, both VOC-sensitive and NO*x*-sensitive regimes are important at Chao-Chou Town. Kenting Town, a touring site at the southern end of Taiwan, was predominated by a NO*x*-sensitive regime in four seasons.

Acknowledgments

This work was supported by the Environmental Protection Bureau, Government of Pingtung County, Taiwan, China. Thanks also go to graduate students Y. T. Huang, F. J. Yang, and S.Y. Liao for their assistance during the course of field measurements.

References

Blanchard C L, 2000. Ozone process insights from field experiments – part III: extent of reaction and ozone formation. *Atmospheric Environment*, 34: 2035–2043.

Chen K S, Ho Y T, Lai C H, Chou Y M, 2003. Photochemical modeling and analysis of meteorological parameters during ozone episodes in Kaohsiung, Taiwan. *Atmospheric Environment*, 37: 1811–1823.

Chen K S, Ho Y T, Lai C H, Tsai Y A, Chen S J, 2004. Trends in concentrations of ground-level ozone and meteorological conditions during high ozone episodes in the Kao-Ping Airshed, Taiwan. *Journal of the Air and Waste Management Association*, 54: 36–48.

Delany A C, Dickerson R R, Melchior Jr F L, Wartborg A F, 1982. Modification of commercial NO*x* detector for high sensitivity. *Review of Scientific Instruments*, 53: 1899–1902.

Dickerson R R, Delany A C, Wartburg A F, 1984. Further modification of a commercial NO*x* detector for high sensitivity. *Review of Scientific Instruments*, 55: 1995–1998.

Fehsenfeld F C, Dickerson R R, Hübler G, Luke W T, Nunnermacker L J, Williams E J et al., 1987. A ground-based intercomparison of NO, NO*x*, and NO*y* measurement techniques. *Journal of Geophysical Research*, 92: 14710–14722.

Hidy G M, 2000. Ozone process insights from field experiments–part I: overview. *Atmospheric Environment*, 34: 2001–2022.

Honrath R E, Jaffe D A, 1990. Measurements of nitrogen oxides in the Arctic. *Geophysical Research Letters*, 17: 611–614.

Hurley P, Manins P, Lee S, Boyle R, Ng Y L, Dewundege P, 2003. Year-long, high-resolution, urban airshed modelling: Verification of TAPM predictions of smog and particles in Melbourne, Australia. *Atmospheric Environment*, 37: 1899–1910.

Hurley P, Blockley J A, Rayner K, 2003. Verification of a prognostic meteorological and air pollution model for year-long predictions in the Kwinana industrial region of Western Australia. *Atmospheric Environment*, 35: 1871–1880.

Hwang M K, Kim Y K, Oh I B, Lee H W, Kim C H, 2007. Identification and interpretation of representative ozone distributions in association with the sea breeze from different synopitic winds over the coastal urban area in Korea. *Journal of the Air and Waste Management Association*, 57: 1480–1488.

Jimenez P, Baldasano J M, 2004. Ozone response to precursor controls in very complex terrains: Use of photochemical indicators to assess O_3-NO*x*-VOC sensitivity in the northeastern Iberian Peninsula. *Journal of Geophysical Research*, 109: D20309.

Lal S K, Akira K, Akikazu K, Yoshio I, 2009. High-resolution modeling and evaluation of ozone air quality of Osaka using MM5-CMAQ system. *Journal of Environmental Sciences*, 21(6): 782–789.

Lin C H, 2008. Impact of downward-mixing ozone on surface ozone accumulation in southern Taiwan. *Journal of the Air and Waste Management Association*, 58: 562–579.

Liu C H, Leung Y C, 2008. Numerical study on the ozone formation inside street canyons using a chemistry box

model. *Journal of Environmental Sciences*, 20 (7): 832–837.

Liu P W G, 2007. Establishment of a bok-jenkins multivariate time-series model to simulate ground-level peak daily one-hour ozone concentrations at ta-liao in Taiwan. *Journal of the Air and Waste Management Association*, 57: 1078–1090.

Milford J B, Gao D, Sillman S, Blossey P, Russel A G, 1994. Total reactive nitrogen (NO*y*) as an indicator of the sensitivity of ozone to reduction in hydrocarbons and NO*x* emissions. *Journal of Geophysical Research*, 99: 3533–3542.

Milford J B, Russell A G, McRae G J, 1989. A new approach to photochemical pollution control: implications of spatial patterns in pollutant responses to reductions in nitrogen oxides and reactive organic gas emissions. *Environment Science and Technology*, 23: 1290–1301.

NRC (National Research Council), 1991. Rethinking the Ozone Problem in Urban and Regional Air Pollution. National Academy Press, Washington, DC.

Occupational Safety and Health Administration (OSHA), 1978. http://www.osha.gov/dts/sltc/methods/inorganic/id006/hydrogen_peroxide.htmls.

Peng Y P, Chen K S, Lai C H, Lu P J, Kao J H, 2006. Concentrations of H_2O_2 and HNO_3 and ozone sensitivity in the ambient air of southern Taiwan. *Atmospheric Environment*, 40: 6741–6751.

Roselle S J, Schere K, 1995. Modeled response of photochemical oxidants to systematic reductions in anthropogenic volatile organic compounds and NO*x* emissions. *Journal of Geophysical Research*, 100: 22929–22941.

Russell A, Dennis R, 2000. NARSTO critical review of photochemical models and modeling. *Atmospheric Environment*, 34: 2283–2324.

Sillman S, 1999. The relation between ozone, NO*x* and hydrocarbons in urban and polluted rural environments. *Atmospheric Environment*, 33: 1821–1845.

Sillman S, 1995. The use of NO*y*, H_2O_2, and HNO_3 as indicators for ozone-NO*x*-hydrocarbon sensitivity in urban locations; *Journal of Geophysical Research*, 100: 14175–14188.

Sillman S, He D, Cardelino C, Imhoff R E, 1997. The use of photochemical indicators to evaluate ozone-NO*x*-hydrocarbon sensitivity: Case studies from Atlanta, New York, and Los Angeles. *Journal of the Air and Waste Management Association*, 47: 1030–1040.

Trainer M, Parrish D D, Buhr M P, Norton R B, Fehsenfeld F C, Anlauf K G et al., 1993. Correlation of ozone with NO*y* in photochemically aged air. *Journal of Geophysical Research*, 98: 2917–2926.

Trainer M, Parrish D D, Goldan P D, Roberts J, Fehsenfeld F C, 2000. Review of observation-based analysis of the regional factors influencing ozone concentrations. *Atmospheric Environment*, 34: 2045–2061.

Williams E, 1995. NO*y* Intercomparison Study, Southern Oxidants Study 1995 Data Analysis Workshop and Annual Meeting. Raleigh, NC.

Willmott C J, Ackleson S G, Davis R E, Feddema J J, Klink K M, Legates D R et al., 1985. Statistics for the evaluation and comparisons of models. *Journal of Geophysical Research*, 90: 8995–9005.